Biological effects of inorganic arsenic on primary cultures of rat astrocytes

IRENE CATANZARO[1*], GABRIELLA SCHIERA[2*], GIULIA SCIANDRELLO[1], GIUSI BARBATA[1], FABIO CARADONNA[1], PATRIZIA PROIA[3] and ITALIA DI LIEGRO[2]

[1]Dipartimento di Biologia Cellulare e dello Sviluppo, [2]Dipartimento di Biomedicina Sperimentale e Neuroscienze Cliniche; [3]Dipartimento di Studi Giuridici, Economici, Biomedici, Psicosociopedagogici delle Scienze Motorie e Sportive, Università degli Studi di Palermo, Palermo, Italy

Received June 29, 2010; Accepted July 26, 2010

DOI: 10.3892/ijmm_00000485

Abstract. It is well established that inorganic arsenic induces neurotoxic effects and neurological defects in humans and laboratory animals. The cellular and molecular mechanisms of its actions, however, remain elusive. Herein we report the effects of arsenite ($NaAsO_2$) on primary cultures of rat astrocytes. Cells underwent induction of heat shock protein 70 only at the highest doses of inorganic arsenic (30 and 60 μM), suggesting a high threshold to respond to stress. We also investigated arsenic genotoxicity with the comet assay. Interestingly, although cells treated with 10 μM arsenite for 24 h maintained >70% viability, with respect to untreated cells, high DNA damage was already observed. Since arsenic is not known to be a direct-acting genotoxic agent, we investigated the possibility that its effects are due, in astrocytes as well, to ROS formation, as already described for other cell types. However, FACS analysis after CM-H_2DCFDA staining did not evidence any significant increase of ROS production while, on the contrary, at the highest arsenite concentrations used, ROS production decreased. Concordantly, we found that, if most cells in the culture are still alive (i.e. up to 10 μM arsenite), they show a treatment-dependent increase in the concentration of SOD1. On the other hand, SOD2 concentration did not change. Finally, we found that astrocytes also synthesize PIPPin, an RNA-binding protein, the concentration of which was recently reported to change in response to stress induced by cadmium. Here we also report that, in cells exposed to high doses of arsenite, an anti-PIPPin antibody-positive faster migrating protein appears.

Correspondence to: Professor Italia Di Liegro, Dipartimento di Biomedicina Sperimentale e Neuroscienze Cliniche, Sezione di Scienze Biochimiche, Via del Vespro 129, I-90127 Palermo, Italy
E-mail: diliegro@unipa.it

*Contributed equally

Key words: inorganic arsenic, astrocytes, cell damage, DNA damage, PIPPin

Introduction

Arsenic is a well known toxic metalloid, widely distributed in nature. It is released into the environment through industrial processes and agricultural usage. Human exposure therefore mainly occurs by consumption of water and food (1,2). Arsenic has been classified as a potent environmental carcinogen for humans (3), inducing a variety of malignancies, especially skin and lung cancers (4). Moreover, arsenic exposure gives rise to cardiovascular diseases and neurological dysfunctions (5).

Although intensively studied, it is not well understood how arsenic acts in living cells, but important insights into the mechanisms that promote arsenic-induced carcinogenesis have been provided by investigations on cultured cells exposed to acute or chronic arsenic treatment. Effects observed just after treatment are aneuploidy and DNA methylation alterations (6). These findings are consistent with a non-mutagenic mode of action and are suggestive of indirect genotoxic mechanisms (7).

Important targets of arsenic appear to be the mitochondria where production of reactive oxygen species (ROS) induces dissipation of mitochondrial transmembrane potential, leading to apoptosis (8,9). In addition, arsenic activates an endoplasmic reticulum (ER) stress-mediated pathway of cell apoptosis (10). These effects could be related with modulations of Ca^{2+}-induced signaling, as recently demonstrated by Florea *et al* (11). Micromolar concentrations of arsenic triggered an increase of intracellular [Ca^{2+}], inhibited cell growth and induced apoptosis in malignant cell lines (12).

Since it has been reported that nonlethal exposure to arsenic induces neurotoxic effects and neurological diseases in humans and laboratory animals (13-16), it is worth studying how arsenic acts on brain cells. The present study was aimed at analyzing the effects of $NaAsO_2$ on primary cultures of rat astrocytes by determining DNA damage by comet assay, and evaluating possible changes of the concentration of the highly conserved heat shock protein 70 (Hsp70) and its housekeeping counterpart, Hsc70. We also investigated the effects of arsenic on PIPPin (also called CSD-C2), a putative RNA-binding protein expressed in the brain and probably involved in the post-transcriptional regulation of genes encoding replacement histones, and in the terminal differentiation of different classes of brain cells (17-19). PIPPin shuttles between the nucleus and cytoplasm, and can undergo post-translational modifications,

such as phosphorylation (18, Di Liegro *et al*, unpublished obserations) and sumoylation (19), in response to extracellular stimuli.

Materials and methods

Animals. Sprague-Dawley rats (Stefano Morini, San Polo d'Enza, Italy) were housed under direction of a licensed veterinary, who also approved the experimental protocols. Procedures involving animals were conducted according to European Community Council Directive 86/609, OJL 5358 1, December 12, 1987.

Cell cultures and arsenic treatment. Astrocytes were prepared from two-day old newborn rats, as previously described (20), and cultured in DME/Hams F-12 (2/1), supplemented with 10% heat-inactivated fetal calf serum (Sigma-Aldrich, MO, USA), until half confluent.

For checking culture purity, astrocytes were cultured on coverslips, fixed with 96% ethanol on ice for 10 min and permeabilized for 5 min with 0.1% Triton X-100 in PBS. Cells were finally incubated with polyclonal rabbit anti-glial fibrillary acidic protein (GFAP) antibodies (Sigma-Aldrich).

Astrocyte cultures were treated with $NaAsO_2$ (Sigma-Aldrich), at final concentrations of 2.5, 5, 10, 30, or 60 μM in complete medium, for 24 h. Arsenite was freshly dissolved in sterile double distilled water.

Acridine orange (AO)/ethidium bromide (EB) assay. Cell death was evaluated by staining astrocytes with AO/EB mixture, each at a concentration of 100 μg/ml in PBS, as previously described (21). Cells were observed by an Olympus BX-50 fluorescent microscope (Olympus Italia SRL, Segrate, Italy).

Trypan blue exclusion test. Treated and untreated cells were stained for 5 min with 0.4% Trypan blue (Sigma-Aldrich), and counted using a Burker chamber under a light microscope with a x20 magnification. The Trypan blue dye is normally taken up by non-viable cells but not by viable cells because it only penetrates through damaged cellular membranes. Cell viability was expressed as the percentage of viable cells compared to the total number of counted cells. Three independent experiments were performed and data are reported as means ± SD.

Alkaline comet assay. Comet assay was performed according to Andreoli (22) with some modifications. Briefly, exponentially growing cells were trypsinized and cell suspension, containing $1x10^6$ cells, was plated in 100-mm petri dishes. After 24 h, cells were treated with increasing doses of $NaAsO_2$ for 24 h, and washed twice with Hank's salt solution. Cells collected by trypsinization were centrifugated at 800 rpm for 10 min, resuspended in PBS ($2x10^5$ cells/10 ml final concentration) and mixed with 65 μl of 0.7% Low Melting Agarose (LMA, Bio-Rad). They were then layered on a slide (GelBond film, Sigma), previously coated with a layer of 0.5% Normal Melting Agarose (NMA, Fisher Molecular Biology), and covered with another layer of LMA. The agarose suspension was covered with a coverslip and placed at 4˚C for 10 min. The coverslip was gently removed and the slide was submerged into lysing solution (2.5 M NaCl, 100 mM Na_2EDTA, 10 mM Tris, 10% DMSO, 1% Triton X-100, pH 10.0) for 1 h in the dark at 4˚C. After lysis, the slides were placed for 15 min in a horizontal electrophoresis gel tray containing fresh alkaline buffer (300 mM NaOH, 1 mM Na_2EDTA, pH >8) and then subjected to an electric field of 0.7 V/cm in the dark at 4˚C for 20 min. Following electrophoresis the microgels were neutralized in 0.4 M Tris-HCl (pH 7.5), dehydrated in methanol for 2 min and allowed to dry at room temperature. The DNA was stained with ethidium bromide (2 μg/ml) (Electran BDH), and visually examined by fluorescence microscope (Nikon Microphot-FXA/SA), equipped with an HBO 100 mercury lamp and a suitable filter. Photomicrographs were processed using Photoshop 6.0 software (Adobe). For qualitative evaluation, at least 1,000 cells were scored for each dose. Cells were classified as undamaged, damaged with comet shape and ghosts with small head and large tails. DNA damage was quantified by tail length values (Ltail, mm) calculated by CASP (Comet Assay Software Project).

Data derived from three independent experiments, with at least 50 cells per experiment (from two replicate slides each), were processed with the Kruskal-Wallis non-parametric statistical method.

ROS detection. Oxidative stress was evaluated using 5-(and-6)-chloromethyl-2'7'-dichloro dihydrofluorescein diacetate acetyl ester (CM-H_2DCFDA, Molecular Probes, Invitrogen). This probe becomes fluorescent when oxidation occurs within the cell.

Experiments were carried out according to the manufacturer's protocol. Briefly, $3x10^6$ exponentially growing astrocytes, immediately after the arsenite treatment, were washed twice with Hank's salt solution, collected by trypsinization and then incubated in the dark with 25 μM CM-H_2DCFDA for 1 h. Finally, they were analysed by flow cytometer (FACScan Becton Dickinson), using excitation sources and filters appropriate for fluorescein (FITC). Treated and untreated cells were evaluated. As positive control, cells were treated for 1 h with 100 μM *tert*-butyl hydroperoxide (TBHP). Experiments were repeated three times.

Western blot analysis. After treatment, astrocytes were collected, washed with PBS, and homogenized in homogenization buffer (0.32 M sucrose; 50 mM sodium phosphate buffer, pH 6.5; 50 mM KCl; 0.5 mM spermine; 0.15 mM spermidine; 2 mM EDTA, and 0.15 mM EGTA), containing the protease inhibitors aprotinin (2 μg/ml), antipain (2 μg/ml), leupeptin (2 μg/ml), pepstatin A (2 μg/ml), benzamidine (1.0 mM), and phenylmethylsulfonyl fluoride (1.0 mM), all purchased from Sigma-Aldrich. Total protein concentration was determined by the Ouant-iT™ Protein Assay using a Qubit™ fluorometer (Invitrogen). Equal amounts of proteins (10-20 μg) were loaded onto each lane of 15% acrylamide-SDS denaturing gels. After electrophoretic separation, samples were electroblotted onto a PVDF membrane (0.45 μm pore-size, Amersham Biosciences). Concentrations of the samples on the membrane were visualized by staining with Ponceau Red for 5 min. Finally, the membrane was immunostained with one of the following antibodies: i) rabbit polyclonal anti-Hsp70 (Calbiochem, Darmstadt, Germany); ii) mouse polyclonal anti-Hsc70 (Santa Cruz, CA, USA); iii) rabbit

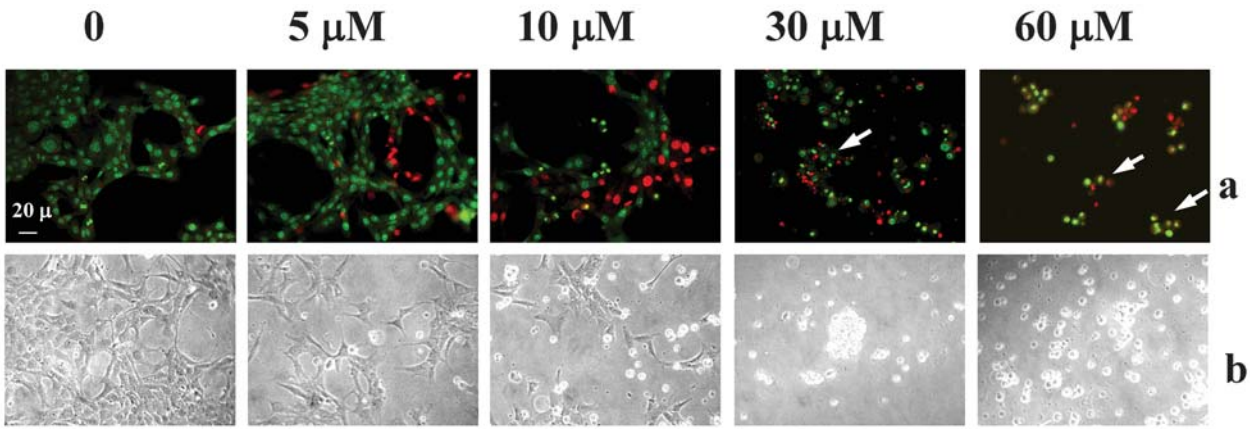

Figure 1. Astrocytes stained with a combination of the fluorescent DNA-binding dyes acridine orange and ethidium bromide. (a) Fluorescent microscopy; (b) light inverted microscopy. Cells were treated with 0, 5, 10, 30 and 60 μM arsenite. Cell cultures were prepared as described in Materials and methods, and treated with arsenite for 24 h. Bar, 20 μ. Arrows indicate putative apoptotic bodies.

Table I. Trypan blue exclusion test after 24 h of sodium arsenite treatment

Arsenite concentration (μM)	Viable cells (%)
0.0	99.0±3.9
2.5	90.0±7.0
5.0	91.9±5.9
10.0	86.4±12.0*
30.0	77.5±8.3*
60.0	63.2±7.8**

Data are the mean of three independent experiments ± SD; *P<0.04 vs control; **P<0.01 vs control, according to the Student's t-test.

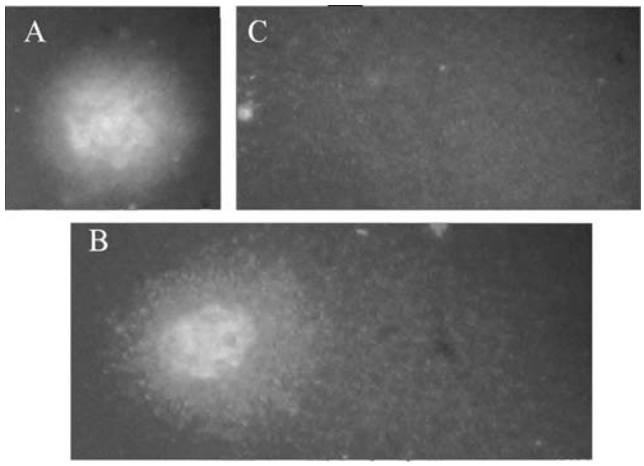

Figure 2. Representative photomicrographs of undamaged (A), damaged (B) and ghost rat astrocytes (C), respectively, after comet assay. Nuclei were stained with ethidium bromide and observed using a fluorescence microscope at x100 magnification.

polyclonal anti-PIPPin antibody, obtained in our laboratory, by immunizing rabbits with recombinant PIPPin, as already described (18); iv) rabbit polyclonal anti-superoxide dismutase 1 (Abcam, Cambridge, UK); v) rabbit polyclonal anti-superoxide dismutase 2 (Abcam). The secondary, anti-rabbit or anti-mouse antibodies were from Promega Corporation (WI, USA). In order to normalize the signals in identical conditions, in most experiments, the membranes were cut into two or even three horizontal stripes, each of which was immunostained with a different antibody. The intensity of bands was evaluated by the ImageJ programme. The measurements obtained from at least 4 independent experiments were finally used to calculate the relative concentrations of the analyzed proteins in the different conditions, as well as standard deviations (SD) and significance of the findings.

Results

Cell viability. For checking culture purity, astrocytes were cultured on coverslips and immunostained as described in Materials and methods. Typically ≥95% of cells were GFAP-positive (data not shown). Light microscopy of cells treated with increasing concentrations of sodium arsenite for 24 h indicated that cells started detaching from lower concentrations of arsenite (5 and 10 mM) and after exposure to 30 and 60 mM arsenite, only ~15% of cells remained attached (Fig. 1b). Also attached cells appeared as increasingly damaged with respect to controls. As shown in Fig. 1a, staining of cells with a mixture of AO and EB demonstrated that the average number of viable (green) cells decreased, indeed, from 94±14 (controls) to 83±10 and 69±25%, after treatment with 5 and 10 mM arsenite, respectively. In cell cultures treated with 30 and 60 μM of arsenite, the toxic effects were very severe and prevented the cell viability evaluation. However, it was possible to see some apoptotic cells (yellow).

Trypan blue exclusion test. As reported in Table I, exposure to 60 μM arsenite resulted in <70% relative viability with respect to control. Thus, this concentration was discarded for the evaluation of DNA damage by comet assay that requires the use of viable cells (23).

Comet assay. To evaluate DNA damage induced in primary cultures of rat astrocytes by exposure to arsenite, we used the comet assay. Preliminary qualitative analyses, performed by classifying cells in three groups, undamaged, damaged and

Table II. Comet assay after 24 h of sodium arsenite treatment.

Arsenite concentration (μM)	Undamaged (%)	Damaged (%)	Ghost (%)
0	85.1±9.5	14.1±10.1	0.7±0.6
2.5	55.2±19.5	42.5±21.1	2.2±0.4
5.0	53.7±29.0	39.6±24.1	6.5±5.1
10	33.4±0.2	43.1±0.7*	23.5±0.9**
30	0	0	100

Data are the mean of three independent experiments + SD; *P<0.05 vs control; **P<<0.01 vs control, according to the Student's t-test.

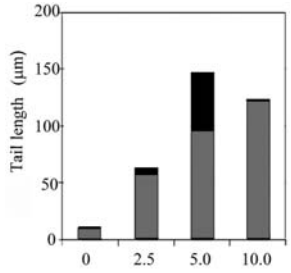

Figure 3. Comet assay, effect of 24 h treatment with 0, 2.5, 5, and 10 μM arsenite on DNA tail length. Grey bars represent the mean of three independent experiments. Black bars are SD. p<0.0001, for all arsenite doses vs. control, according to Kruskal-Wallis test.

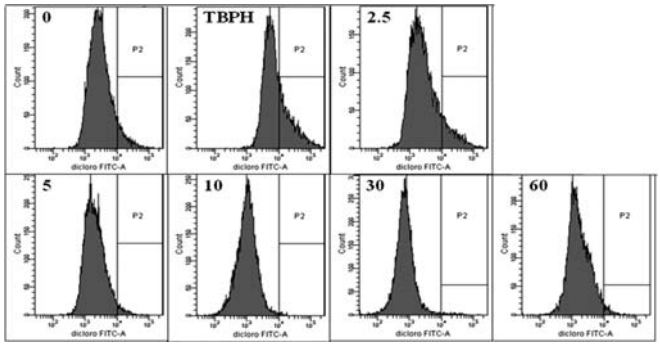

Figure 4. Fluorescence-activated cell sorting (FACS) histograms show the effects on astrocytes after treatment with different doses of arsenite (0, 2.5, 5, 10, 30 and 60 μM) for 24 h. Oxidative stress was evaluated using CM-H_2DCFDA. As a positive control, astrocytes were also treated with 100 μM TBHP. The histograms shown are representative of three independent experiments.

ghost cells (Fig. 2), revealed a significant dose-dependent increase of damaged and ghost cells (Table II). Quantitative evaluation, performed by CASP in cells exposed to 2.5, 5.0 and 10.0 μM, revealed a significant increase of the tail length in comparison with untreated cells (Fig. 3).

ROS detection. We assessed ROS levels in arsenite-treated astrocytes by measuring with flow cytometry their ability to oxidize the fluorogenic dye CM-H_2DCFDA. The effect of arsenite treatment on the FACS histograms was not significant. However, at the highest doses of arsenite, a trend to a leftward shift was noted, indicating a lower degree of dye oxidation. For example, 10 μM arsenite resulted in 35.54% decrease in fluorescence (Fig. 4). On the other hand, histograms of astrocytes treated with 100 μM TBHP (positive control) show a clear rightward shift, indicating a greater oxidation of the dye.

Western blot analyses. We then analyzed the expression of stress proteins in astrocytes treated with increasing amounts of arsenite. As shown in Fig. 5, cells treated with 30-60 μM arsenite (i.e. cells which lost their normal morphology, Fig. 1), express high levels of the stress protein Hsp70, whereas they do not show any change in Hsp70 levels at lower arsenite concentrations. On the other hand, cells do not undergo any change in the housekeeping Hsc70 levels, at any arsenite concentration. We also studied the effect of arsenite on the expression of superoxide dismutases 1 and 2 (SOD1 and SOD2). As shown in Fig. 6, a slight, arsenite concentration-dependent, increase of SOD1 is evident up to 10 μM arsenite (i.e. when cells still maintain normal morphology even if signs of cell damage are already evident, Fig. 1), while a decrease

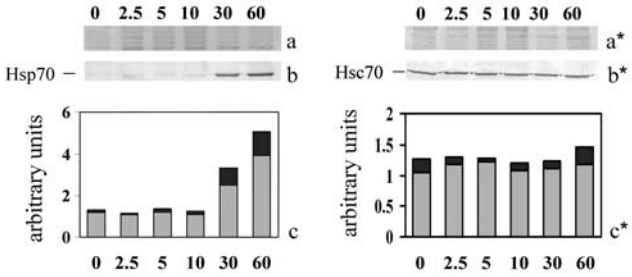

Figure 5. Western analysis of total cell proteins from astrocytes, treated with 0, 2.5, 5, 10, 30, or 60 μM arsenite, for 24 h. Total proteins from cell lysates were immunostained with rabbit polyclonal anti-Hsp70 (Calbiochem, Darmstadt, Germany) antibodies (b), or mouse polyclonal anti-Hsc70 (Santa Cruz, CA, USA) antibodies (b*). Ponceau red-stained regions of the same membranes used for the Western blot analyses are shown in a, and a*, respectively. At least three independent Western blots were scanned and analyzed with the ImageJ program. The results were used to calculate mean relative concentrations of the proteins of interest (c, and c*). Grey and black bars in c and c* indicate mean values and SD, respectively.

was observed at higher arsenite concentrations. No significant change of SOD2 was noted at any arsenite concentrations.

Finally, we analyzed the expression levels of RNA-binding protein PIPPin. As shown in Fig. 7, the expected main band of ~30 kDa increased at intermediate doses (5 μM) of arsenite and decreased at the highest doses (30 and 60 μM) while, in parallel, a faster migrating band appeared of ~28 kDa.

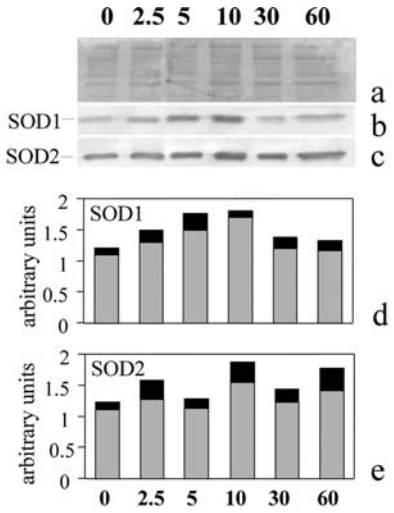

Figure 6. Western analysis of total cell proteins from astrocytes, treated with 0, 2.5, 5, 10, 30, or 60 μM arsenite, for 24 h. Total proteins from cell lysates were immunostained with rabbit polyclonal anti-SOD1 (b) or anti-SOD2 (c) antibodies. A Ponceau red-stained region of the same membrane, used for Western blot analyses, is shown in a. At least three independent Western blots were scanned and analyzed with the ImageJ program. The results were used to calculate mean relative concentrations of the proteins of interest (d and e, respectively). Grey and black bars indicate mean values and SD, respectively.

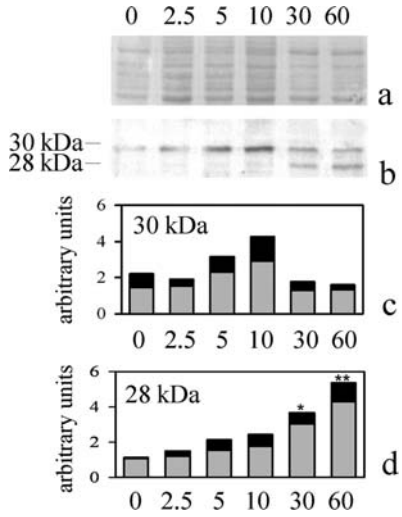

Figure 7. Western blot analysis of total cell proteins from astrocytes, treated with 0, 2.5, 5, 10, 30, or 60 μM arsenite, for 24 h. Proteins were immunostained with rabbit polyclonal anti-PIPPin antibodies (b). A Ponceau red-stained region of the same membrane used for Western blot analysis is shown in a. At least three independent Western blots were scanned and analyzed with the ImageJ program. The results were used to calculate mean relative concentrations of both 30- and 28-kDa proteins (c and d, respectively). Grey and black bars indicate mean values and SD, respectively. $^{*}p<0.025$ vs control, and $^{**}p<0.01$ vs control, respectively, according to the Student's t-test.

Discussion

Chronic exposure to arsenic at nonlethal levels can result in a variety of outcomes including cognitive impairment (1). Neurotoxic effects have been reported both in clinical cases and animal experiments. It has been demonstrated that arsenic induces decreased locomotor activity and behavioral disorders in exposed male rats (15), and that the effects can be transmitted from the maternal to fetal tissues across the transplacental barrier (14).

Astrocytes, the most abundant glial cell population in the central nervous system (CNS), contribute to the establishment of the blood-brain barrier (24, and references therein), and perform functions particularly important in maintaining neuronal viability (25). Moreover, astrocytes form the front line in the brain parenchyma against foreign molecules crossing the blood-brain barrier. However, information on the putative ability of astrocytes in protecting neurons from arsenite toxicity is still scarce. Understanding the biochemical mechanisms of astrocyte response to the metalloid is thus of crucial importance for gaining further insights into the effects arsenic has on CNS.

In the present study, the exposure to micromolar concentrations of arsenite induced in primary cultured rat astrocytes both morphological and biochemical changes. As indicated by AO/EB tests, most cells died at the highest doses of arsenite (30-60 μM), and 20-30% of cells already underwent damage at lower arsenite concentrations (5-10 μM). The percentage of suffering cells, however, is clearly higher, as demonstrated by directly looking at DNA damage by the comet assay (only ~33% of cells still undamaged at 10 μM arsenite). On the basis of these findings we should have expected an increase of ROS production in treated astrocytes, since on one hand, arsenic is known to induce modifications of ROS levels in other cell types (26), and, on the other, astrocytes are known to respond to certain stress with an increase of ROS production (25,27). However, arsenite treatment did not induce increased ROS levels in astrocytes, but on the contrary a decrease, suggesting the occurrence of some modifications which result in a generally decreased rate of basal metabolism. A parallel slight increase of expression of SOD1 was found while cells were still resistant to the treatment (up to 10 μM arsenite). On the other hand, even SOD1 decreased when cells are definitively damaged. Curiously, the mitochondrial SOD2 did not undergo any significant changes.

In the absence of ROS production, it is possible that the DNA damage evidenced by the comet assay is instead due to the production of trivalent methylated arsenic metabolites, which have been reported to be more toxic than arsenite both *in vitro* and *in vivo*, and capable of inducing DNA alkali-labile sites (26).

The only clear modification in the levels of proteins linked to stress was the highly significant increase of Hsp70, at the highest doses of arsenite (30 and 60 μM). This finding suggests that astrocytes sense arsenite exposure as a stress only at very high doses, when most cells are already too damaged to survive. It is probable that cells expressing Hsp70 are still alive even at the highest doses of arsenite.

Since other authors reported that the effects of arsenite could relate to modulations of Ca^{2+}-induced signaling (11,12), we also analyzed the effects of arsenite treatment on PIPPin, a putative RNA-binding protein (also known as CSD-C2), the concentration of which was recently found to decrease when neurons undergo a cadmium-induced stress (28). PIPPin is most closely related to CRHSP24, a protein particularly abundant in the pancreas, testis, liver, and lung, which has been suggested to be involved in calcium-mediated signal transduction (29,30). First, we explored if PIPPin is also expressed

in primary cultures of astrocytes and found that it is, even at lower levels with respect to neurons (data not shown). Second, we looked for modifications of its levels after arsenite treatment. Such as in the case of cadmium-induced stress (28), PIPPin concentration changes only at the highest doses of arsenite. In arsenite-treated astrocytes, however, we found a dose-dependent increase of a faster migrating protein, also stained by anti-PIPPin antibodies. The origin of this protein is still under analysis, but we hypothesize that it derives from a proteolytic event connected with stress-induced cell death.

In conclusion: i) arsenite exposure causes damage to astrocytes by a process not involving oxidative stress; ii) astrocytes appear to have a very high threshold for induction of stress proteins, such as Hsp70, a well known marker of cell stress, that does not increase until cells are exposed to very high concentrations of arsenite; iii) astrocytes express PIPPin; iv) arsenite exposure induces in rat astrocytes the production of a novel form of PIPPin, the analysis of which could shed further light on PIPPin involvement in stress response.

Acknowledgements

This work was entirely supported by the University of Palermo (Fondi di Ateneo, Università degli Studi di Palermo). I. Catanzaro and G. Schiera were supported by postdoctoral fellowships by Università degli Studi di Palermo, Palermo, Italy.

References

1. Kapaj S, Peterson H, Liber K and Bhattacharya P: Human health effects from chronic arsenic poisoning - a review. J Environ Sci Health A Tox Hazard Subst Environ Eng 41: 2399-2428, 2006.
2. Singh N, Kumar D and Sahu AP: Arsenic in the environment: effects on human health and possible prevention. J Environ Biol 28: 359-365, 2007.
3. IARC (International Agency for Research on Cancer): IARC Monographs on the Evaluation of the Carcinogenic Risk of Chemicals to Humans 23: Some Metals and Metallic Compounds. World Health Organization, Lyon, 1980.
4. Kitchin KT: Recent advances in arsenic carcinogenesis: modes of action, animal model systems, and methylated arsenic metabolites. Toxicol Appl Pharmacol 172: 249-261, 2001.
5. Chen Y, Parvez F, Gamble M, Islam T, Ahmed A, Argos M, Graziano JH and Ahsan H: Arsenic exposure at low-to-moderate levels and skin lesions, arsenic metabolism, neurological functions, and biomarkers for respiratory and cardiovascular diseases: review of recent findings from the Health Effects of Arsenic Longitudinal Study [HEALS] in Bangladesh. Toxicol Appl Pharmacol 239: 184-192, 2009.
6. Sciandrello G, Caradonna F, Mauro M and Barbata G: Arsenic-induced DNA hypomethylation affects chromosomal instability in mammalian cells. Carcinogenesis 25: 413-417, 2004.
7. Klein CB, Leszczynska J, Hickey C and Rossman TG: Further evidence against a direct genotoxic mode of action for arsenic-induced cancer. Toxicol Appl Pharmacol 222: 289-297, 2007.
8. Haga N, Fujita N and Tsuruo T: Involvement of mitochondrial aggregation in arsenic trioxide [As_2O_3]-induced apoptosis in human glioblastoma cells. Cancer Sci 96: 825-833, 2005.
9. Liu SX, Davidson MM, Tang X, Walker WF, Athar M, Ivanov V and Hei TK: Mitochondrial damage mediates genotoxicity of arsenic in mammalian cells. Cancer Res 65: 3236-3242, 2005.
10. Du Y, Wang K, Fang H, Li J, Xiao D, Zheng P, Chen Y, Fan H, Pan X, Zhao C, Zhang Q, Imbeaud S, Graudens E, Eveno E, Auffray C, Chen S, Chen Z and Zhang J: Coordination of intrinsic, extrinsic, and endoplasmic reticulum mediated apoptosis by imatinib mesylate combined with arsenic trioxide in chronic myeloid leukemia. Blood 107: 1582-1590, 2006.
11. Florea AM, Splettstoesser F and Büsselberg D: Mechanisms of arsenic trioxide [As_2O_3] induced calcium signals and cellular death in two human SY-5Y neuroblastoma and 293 embryonic kidney [HEK] cells. Toxicol Appl Pharmacol 220: 292-301, 2007.
12. Zhang TC, Cao EH, Li JF, Ma W and Qin JF: Induction of apoptosis and inhibition of human gastric cancer MGC-803 cell growth by arsenic trioxide. Eur J Cancer 35: 1258-1263, 1999.
13. Rodríguez VM, Carrizales L, Jiménez-Capdeville ME, Dufour L and Giordano M: The effects of sodium arsenite exposure on behavioral parameters in the rat. Brain Res Bull 55: 301-308, 2001.
14. Chattopadhyay S, Bhaumik S and Nag-Chaudhury A: Arsenic induced changes in growth development and apoptosis in neonatal and adult brain cells in vivo and in tissue culture. Toxicol Lett 128: 73-84, 2002.
15. Rodriguez VM, Carrizales L and Mendoza MS: Effects of sodium arsenite exposure on development and behavior in the rat. Neurotoxicol Teratol 24: 743-750, 2002.
16. Ratnaike RN: Acute and chronic arsenic toxicity. Postgrad Med J 79: 391-396, 2003.
17. Castiglia D, Scaturro M, Nastasi T, Cestelli A and Di Liegro I: PIPPin, a putative RNA-binding protein specifically expressed in the rat brain. Biochem Biophys Res Commun 218: 390-394, 1996.
18. Nastasi T, Scaturro M, Bellafiore M, Raimondi L, Beccari S, Cestelli A and Di Liegro I: PIPPin is a brain-specific protein that contains a cold-shock domain and binds specifically to H1° and H3.3 mRNAs. J Biol Chem 274: 24087-24093, 1999.
19. Bono E, Compagno V, Proia P, Raimondi L, Schiera G, Favaloro V, Campo V, Donatelli M and Di Liegro I: Thyroid hormones induce sumoylation of the cold shock domain-containing protein PIPPin in developing rat brain and in cultured neurons. Endocrinology 148: 252-257, 2007.
20. Proia P, Schiera G, Mineo M, Ingrassia AMR, Santoro G, Savettieri G and Di Liegro I: Astrocytes shed extracellular vesicles that contain fibroblast growth factor-2 and vascular endothelial growth factor. Int J Mol Med 21: 63-67, 2008.
21. Schiera G, Proia P, Alberti C, Mineo M, Savettieri G and Di Liegro I: Neurons produce FGF2 and VEGF and secrete them at least in part by shedding extracellular vesicles. J Cell Mol Med 11: 1384-1394, 2007.
22. Andreoli C, Leopardi P and Crebelli R: Detection of DNA damage in human lymphocytes by alkaline single cell gel electrophoresis after exposure to benzene or benzene metabolites. Mutat Res 377: 95-104, 1997.
23. Tice RR, Agurell E, Anderson D, Burlinson B, Hartmann A, Kobayashi H, Miyamae Y, Rojas E, Ryu J-C and Sasaki YF: The single cell gel/Comet assay: guidelines for in vitro and in vivo genetic toxicology testing. Environ Mol Mutagen 35: 206-221, 2000.
24. Schiera G, Sala S, Gallo A, Raffa MP, Pitarresi GL, Savettieri G and Di Liegro I: Permeability properties of a three-cell type in vitro model of blood-brain barrier. J Cell Mol Med 9: 373-379, 2005.
25. Wang C-C, Fang K-M, Yang C-S and Tzeng S-F: Reactive oxygen species-induced cell death of rat primary astrocytes through mitochondria-mediated mechanism. J Cell Biochem 107: 933-943, 2009.
26. Rossman TG: Mechanism of arsenic carcinogenesis: an integrated approach. Mutat Res 533: 37-65, 2003.
27. Yang C-S, Tzou B-C, Liu Y-P, Tsai M-J, Shyue S-K and Tzeng S-F: Inhibition of cadmium-induced oxidative injury in rat primary astrocytes by the addition of antioxidants and the reduction of intracellular calcium. J Cell Biochem 103: 825-834, 2008.
28. Gerspacher C, Scheuber U, Schiera G, Proia P, Gygax D and Di Liegro I: The effect of cadmium on brain cells in culture. Int J Mol Med 24: 311-318, 2009.
29. Groblewski GE, Yoshida M, Bragado MJ, Ernst SA, Leykan J and Williams JA: Purification and characterization of a novel physiological substrate for calcineurin in mammalian cells. J Biol Chem 273: 22738-22744, 1998.
30. Auld G, Campbell DG, Morrice N and Cohen P: Identification of calcium-regulated heat-stable protein of 24 kDa [CRHSP24] as a physiological substrate for PKB and RSK using KESTREL. Biochem J 389: 775-783, 2005.